



**This is a postprint of an article published in
Leonhäuser, J., Wang, W., Deckwer, W.-D., Wagner-Döbler, I.
Functioning of the mercury resistance operon at extremely high Hg(II)
loads in a chemostat: A proteome analysis
(2007) Journal of Biotechnology, 132 (4), pp. 469-480.**

Functioning of the Mercury Resistance Operon at Extremely High Hg(II) loads in a Chemostat: A Proteome Analysis

Johannes Leonhäuser^{1§}, Wei Wang^{1§}, Wolf-Dieter Deckwer¹, Irene Wagner-Döbler^{2,*}

1. Technical University Braunschweig / HZI – Helmholtz Center for Infection Research

Biochemical Engineering

Inhoffenstrasse 7

D-38124 Braunschweig, Germany

2. HZI – Helmholtz Centre for Infection Research, Division of Cell Biology

Inhoffenstrasse 7

D-38124 Braunschweig, Germany

[§]Authors equally contributed

* To whom all correspondence should be addressed:

HZI, Inhoffenstrasse 7, D-38124 Braunschweig, Germany

E-mail: irene.wagner-doebler@helmholtz-hzi.de

+ in memory of Prof. W.-D. Deckwer

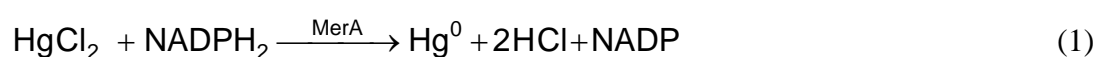
Abstract

The transformation of extremely high concentrations of ionic mercury (up to 500 mg L⁻¹) was investigated in a chemostat for two mercury-resistant *Pseudomonas putida* strains, the sediment isolate Spi3 carrying a regulated mercury resistance (*mer*) operon, and the genetically engineered strain KT2442::*mer73* expressing the *mer* operon constitutively. Both strains reduced Hg(II) with an efficiency of 99.9 % even at the maximum load, but the concentration of particle bound mercury in the chemostat increased strongly. A proteome analysis using two-dimensional gel electrophoresis and mass spectrometry (2-DE/MS) showed constant expression of the MerA and MerB proteins in KT2442::*mer73* as expected, while in Spi3 expression of both proteins was strongly dependent on the Hg(II) concentration. The total cellular proteome of the two strains showed very little changes at high Hg(II) load. However, certain cellular responses of the two strains were identified, especially in membrane-related transport proteins.. In Spi3, an up to 45-fold strong induction of a cation efflux transporter was observed, accompanied by a drastic downregulation (106-fold) of an outer membrane porin. In such a way, the cell complemented the highly specific mercury resistance mechanism with a general detoxification response. No indication of a higher demand on energy metabolism could be found for both strains.

Key words: mercury, biotransformation, proteome analysis

Introduction

Mercury (Hg) is a toxic pollutant widespread in the environment. Mercury has in the past been extensively used in industrial applications (chloroalkali-electrolysis, fungicides, disinfectants, dental products etc.), resulting in local hot spots of pollution and serious effects on biota and humans (Heaven et al., 2000). At present, emissions of Hg into the environment are mainly caused by combustors and power stations (EPA, 1997). As in 1995 burning of fossil fuels was responsible for 77% (1474.5 t/a) of worldwide Hg emissions (European Union, 2001). However, mercury has not entered the environment recently as the results of anthropogenic activities, but has always been a natural component of minerals (e.g. as cinnabar ore) and reaches high concentrations in certain geological formations, e.g. volcanos and hydrothermal vents. Thus, to deal with the presence of mercury in their natural habitats, many microorganisms have evolved an effective resistance mechanism based on the enzymatic transformation of Hg(II) into metallic mercury (Hg(0)). Hg(0) is not toxic for microorganisms and leaves the microbial cell by diffusion. The reductive transformation occurs inside the microbial cell and requires biochemical reduction equivalents (NADPH₂).



The reaction is catalyzed by the enzyme mercury reductase, the product of the *merA* gene. In addition to the *merA* gene, the microbial mercury resistance operon (*mer* operon) contains genes for uptake of mercury compounds, as well as regulatory genes, and in some bacteria also a gene for cleavage of organic mercury compounds. The *merT* and *merP* gene products are transport proteins mediating the transfer of Hg(II) across the periplasmic space and the cytoplasm membrane. *merB* encodes the mercuric lyase, which cleaves the Hg-C-bonds in organomercurials (broad spectrum resistance). The expression of the operon is regulated by the gene products of *merR* and *merD* and is inducible by Hg(II). The product of *merR* represses the expression of the operon in the absence of inducer. The product of *merD*

coregulates the expression of the operon. Truncation of the *merR* gene resulted in recombinant strains which express mercury resistance constitutively (Horn et al., 1994). Details of the resistance mechanism and the structure and function of the involved genes can be found in the literature (Barkay and Wagner-Döbler, 2005, Barkay et al., 2003, Nies, 1999). The regulation of the *mer* operon has been studied in depth (Barkay et al., 2003, Silver and Phung, 1996, Misra, 1992). However, the total cellular response of a resistant microorganism to high Hg(II) loads has not yet been studied.

The aim of this study was to investigate the cellular responses of two mercury-resistant strains of *Pseudomonas putida* to high Hg(II) loads with the help of proteome analysis. The strain Spi3 was isolated from polluted sediments and has a mercury inducible *mer* operon, while the strain KT2442::*mer73* is a genetically engineered strain. For its construction, the *TPAB* genes of the *mer* operon of the mercury-resistant strain *Serratia marcescens* were inserted into the chromosome of *P. putida* KT2440 which is not mercury resistant. . The regulatory genes *merR* and *merD* were removed. Therefore, expression of mercury resistance in KT2442::*mer73* is expected to be independent of mercury and remain constant throughout growth. In addition to a comparison of the gene expression of their *mer* operons, differences between the proteome of these two strains at high mercury load should provide first insights into the total cellular response to mercury in an organism with regulated mercury resistance mechanism (Spi3) compared to an organism with highly expressed resistance mechanism (KT2442::*mer73*). The experiments were performed in chemostat cultures where steady state conditions were obtained that enabled proteome analysis based on stable cell physiologies of homogenous microbial populations. In addition, extreme Hg(II) loads (up to 500 mg L⁻¹) could be applied.

Materials and methods

Strains and medium

The mercury-resistant strains used in this study were *P. putida* KT2442::*mer73*, a genetically engineered strain and *P. putida* Spi3, a naturally mercury-resistant isolate. The construction and characteristics of KT2442::*mer73* are described by Horn et al. (1994). This strain carries a chromosomal insertion of the broad spectrum mercury resistance genes *merTPAB* from *Serratia marcescens*. It is able to reduce ionic mercury as well as organomercurials. The *TPAB* genes were inserted into the alanyl-tRNA-synthase gene and hence are expressed independently of the presence of Hg(II) at a high rate under the control of the constitutive t-RNA synthase promoter (Pauling, 2003).

Pseudomonas putida Spi 3 was isolated from sediments of the Spittelwasser river, a tributary of the Elbe river (von Canstein et al., 1999). The isolate was identified by the DSMZ as *Pseudomonas putida* strain on the basis of 16S rRNA gene sequencing and phenotypical tests. The presence of the *merA* (Felske et al., 2003) and *merB* genes was confirmed by specific PCR with conserved primers based on the alignment of *merA* sequences in the GenBank database (Fehr, 2006). The strain Spi3 contains the regulatory proteins *merR* and *merD* and therefore it expresses mercury resistance only after induction by mercury.

For the cultivation a standard defined minimal medium (M9) was used, containing the following components (per litre): 8.9 g Na₂HPO₄·2H₂O, 2.99 g KH₂PO₄, 0.5 g NaCl, 1.0 g NH₄Cl, 2.5 mL trace element solution. The trace element solution contains (per litre): 0.72 g ZnSO₄·7H₂O, 0.56 g MnSO₄·4H₂O, 0.125 g CuSO₄·5H₂O, 0.095 g CaSO₄·2H₂O, 0.03 g H₃BO₃·4H₂O, 25.6 mL HCl (37%), 30.3 g MgSO₄, 2.5 g FeSO₄·7H₂O (adjusted to pH 2). As a carbon source, glucose (4 g L⁻¹) was added. The MgSO₄ and FeSO₄ solutions were prepared separately and fresh before adding to the other trace element solution. The medium was adjusted to pH 7 with 5 M NaOH solution. The phosphate buffer components of the medium were sterilized (121°C, 20 min.) separately. Trace elements and glucose were filter-sterilized.

Cultivation conditions and bioreactor setup

Continuous cultivation was carried out with a working volume of 1.0 L in a 1.5-L bioreactor (ISF 100 Laboratory Table Fermenter, Infors, Germany) at 30°C. The temperature, oxygen concentration and the pH were controlled and regulated automatically. Figure 1 gives a scheme of the experimental setup. Chemostat cultivations were performed at dilution rates from $D = 0.1 - 0.3 \text{ h}^{-1}$. The working volume was kept constant by peristaltic pumps (202U/AA12, Watson Marlow, USA) which were used for the feeding of the medium and the removal of the culture. The M9 medium and the mercury solution were fed separately. The mercury was fed from an HgCl_2 stock solution which was 10 times concentrated than the final Hg concentration. Therefore, the M9 medium was concentrated 10% more so that the medium flow could be diluted with the mercury flow 10:1 (v/v) before it entered the bioreactor. The chemostat was run for at least five volume changes to reach a metabolic steady state. Samples of 50 mL were taken at regular intervals by collecting the ice cooled effluent during a time period of 30 min. The outlet gas was fed to a Hg vapour absorption system which consisted of two 1-litre washing bottles filled with a mixture of 9 M H_2SO_4 and 0.2 M KMnO_4 (1:5 (v/v)). The reactor and tubing were sterilized by autoclaving at 121°C for 20 min.

To prepare the inoculum, one colony of Spi3 and KT2442::*mer73*, respectively, was picked from a plate, suspended in 100 mL M9 medium and grown at 30°C on a rotary shaker for 24 hours. After 6 hours 1 mg L^{-1} of Hg(II) was added to the inoculum. The inoculum was added under sterile conditions into the reactor to 900 mL of M9 medium.

Analytical procedures

Cell biomass was monitored by measuring the optical density at 600 nm in triplicates with an Ultraspec 3100pro spectrophotometer (Amersham Pharmacia, UK). For the determination of the bio dry mass (BDM), cell pellet from a 2 mL sample was washed and dried in pre-weighted Eppendorf tubes to constant mass at 45°C under vacuum. For the

determination of the D-glucose concentration, 0.1 mL sample was treated with a standard test kit (r-biopharm, Boehringer Mannheim, Germany) and analyzed by an UV method.

The total amount of mercury constituted from soluble and bound Hg was determined by flameless cold vapour adsorption spectroscopy using a flow injection system (FIAS 200, Perkin Elmer) connected to an atomic adsorption spectrophotometer (AAS 2100, Perkin Elmer). To determine the total mercury concentrations, 1 mL of each sample was first oxidized with 150 μL KMnO_4 (5%), 10 μL H_2SO_4 (96%) and 10 μL HNO_3 (65%). 2 minutes later, 100 μL $\text{K}_2\text{S}_2\text{O}_8$ (potassium persulfate, 4%) was added and mixed for further oxidation. After another 10 minutes 230 μL H_3NOHCl (hydroxylammonium chloride, 10%) was added and mixed until the sample was decolorized. Subsequently, the sample was diluted with deionized water to a Hg concentration below 100 $\mu\text{g L}^{-1}$ (maximum value of calibration) and injected into the FIAS. Ionic mercury Hg(II) was reduced to metallic mercury Hg(0) by the addition of NaBH_4 (0.2%). Hg(0) was volatilized by the carrier gas argon and detected at 253.7 nm by the AAS. To measure the soluble Hg concentration ($c_{\text{Hg,S}}$) samples were centrifuged at 6,000 g for 15 min and the supernatants were measured as described above.

Proteome analysis by 2-DE/MS

For proteome analysis 2 x 25 mL of ice cold effluent was immediately centrifuged at 6,000 g and 4°C for 15 min. Cell pellets were washed three times with PBS buffer (93.2 mM Na_2HPO_4 , 6.8 mM NaH_2PO_4 , 100 mM NaCl , pH 7.4) and stored at -80°C for later use. Proteins coded by the genes of the *mer* operon were of special interest for this study. According to their theoretical *pI*, molecular weight (*Mr*) and grand average of hydropathicity (GRAVY) values (Table 1) MerT and MerP are very small basic proteins, and as membrane-bound proteins quite hydrophobic, especially MerT. Therefore, to capture such hydrophobic proteins, a lysis buffer with strong solubility for hydrophobic proteins was needed for 2-D gel electrophoresis. To this end the most commonly used zwitterionic surfactant 3-(3-

cholamidopropyl)-dimethylammonio propane sulfonate (CHAPS) was used in combination with another zwitterionic surfactant aminosulfobetaine-14 (ASB-14) as well as the non-ionic surfactant triton X-100 for enhanced protein solubility. Cell pellets resuspended in this lysis buffer were sonicated to obtain the crude intracellular protein extracts, which were further purified by phenol precipitation/acetone extraction according to the method described before (Wang, et al., 2005).

Combined 2-DE/MS was performed according to the method described in detail by Wang et al. (2005, 2006). For the first dimension isoelectric focussing (IEF), in addition to the IPG strip of pH 4-7 which is normally used to recover most intracellular proteins, IPG strips of pH 6-11 were also used to detect more basic proteins such as MerT and MerP. All samples were analyzed in duplicates. A total protein amount of 150 µg was applied to each IPG strip by in-gel rehydration for pH 4-7 and anodic cup load for pH 6-11 according manufacturer's instruction (GE healthcare). Self-cast acrylamide gels (12.5%) were used for the second dimension SDS-PAGE. For protein spots detection and quantification of protein expressions, gels were stained with fluorescence dye according to the improved fluorescent staining method described by Lamanda et al. (2004) using ruthenium II tris-bathophenanthroline disulfonate (RuBPS), which was prepared according to the method described by Rabilloud et al. (2001).

Protein spots were excised and subjected to in-gel digestion with trypsin, then analyzed by MALDI-TOF MS with a Bruker Ultraflex time-of-flight mass spectrometer (Bruker Daltonics GmbH, Germany). Peptide masses obtained from MALDI-TOF MS analysis were used for protein identification by peptide mass fingerprinting (PMF) against the the specific protein database of *P. putida* KT2442.

Results and Discussion

Hg(II) transformation by *P. putida* KT2442::*mer73* in continuous culture

The strain *P. putida* KT2442::mer73 was cultivated in aerobic chemostats with glucose (4 g L^{-1}) as the sole carbon source at dilution rates of $D = 0.1 - 0.3 \text{ h}^{-1}$. No remaining glucose was found in the effluent, confirming the C-limited cultivation. The biomass yield on glucose $Y_{X/S}$ was about $0.4 \text{ g}_{\text{Biodrymass}} \text{ g}^{-1}_{\text{glucose}}$. Hg(II) inflow concentration $c_{\text{Hg,in}}$ was varied between $10 - 400 \text{ mg L}^{-1}$. The results are shown in Figure 2. At an inflow mercury concentration of 10 mg L^{-1} the total Hg concentration in the effluent ($c_{\text{Hg,T,out}}$) was $50 - 100 \text{ } \mu\text{g L}^{-1}$. The soluble Hg concentration in the effluent after centrifugation ($c_{\text{Hg,S,out}}$) was only $7 - 20 \text{ } \mu\text{g L}^{-1}$, indicating that most mercury was particle bound and therefore not bioavailable. Mercury removal efficiency, calculated between $c_{\text{Hg,in}}$ and $c_{\text{Hg,S,out}}$, was 99.8%.

With an increased Hg(II) inflow concentration of 50 mg L^{-1} the $c_{\text{Hg,T,out}}$ increased to $100 - 200 \text{ } \mu\text{g L}^{-1}$ and the $c_{\text{Hg,S,out}}$ to approx. $50 \text{ } \mu\text{g L}^{-1}$. A further increase of $c_{\text{Hg,in}}$ to 100 mg L^{-1} and later to 200 mg L^{-1} showed no significant differences in $c_{\text{Hg,T,out}}$ and $c_{\text{Hg,S,out}}$. The corresponding mercury removal efficiency was 99.8% and 99.9%, respectively. When $c_{\text{Hg,in}}$ was increased to 400 mg L^{-1} a noticeable increase of $c_{\text{Hg,T,out}}$ to 10 mg L^{-1} was observed. However, $c_{\text{Hg,S,out}}$ of 0.2 mg L^{-1} was significantly lower than $c_{\text{Hg,T,out}}$ and the bio dry mass (BDM) concentration as well as the oxygen consumption remained constant, indicating that the microbial cells were still alive and able to cope with such high Hg(II) loads. Later when $c_{\text{Hg,in}}$ was reduced again the outflow concentration of mercury decreased but did not reach the low values achieved before at similar values of $c_{\text{Hg,in}}$. This was also observed previously, when *P. putida* was applied for mercury removal in a three-phase fluidized bed in repeated batch runs (Becker, 1996). It may be caused by the adsorption of Hg(II) to the outer cell membrane under extreme Hg(II) loads, resulting in a transport resistance for soluble mercury of the cell membrane partly loaded by adsorbed Hg(II).

At day 34 the mercury feed was stopped, but even after 18 exchanges of the chemostat volume as much as $100 \text{ } \mu\text{g L}^{-1}$ of total mercury could still be detected in the effluent ($20 \text{ } \mu\text{g L}^{-1}$

¹ soluble Hg). This was due to the fact that a biofilm had been observed to grow on the reactor wall during the 40 days of operation which adsorbed mercury and released it gradually.

The results are summarized in Table 2. The Hg removal rate was 99.8% or even higher at all dilution rates and up to an inflow concentration of 200 mg L⁻¹. Due to these high conversion efficiencies the volumetric transformation rate was only proportional to the Hg(II) load, given by

$$R_{\text{Hg},V} = D (c_{\text{Hg},\text{in}} - c_{\text{Hg},\text{out}}) \approx D c_{\text{Hg},\text{in}} \quad (2)$$

The same general trend was found for the specific rate $R_{\text{Hg},X}$.

Generally a large difference was found between the total mercury concentration versus the soluble Hg concentration in the effluent. Mercury can easily bind to microbial cells with high affinity, as evidenced by data on the adsorption of HgCl₂ to the non-mercury-resistant *P. putida* KT2442 reported before (Deckwer et al., 2004). Typical Langmuir adsorption behaviour was found with a maximal load of $q_{\text{max}} = 200 \mu\text{g Hg(II) mg}^{-1} \text{BDM}$ and an adsorption equilibrium constant of $K_A = 0.8 \text{ L mg}^{-1}$. These adsorption results are in agreement with those found with another *P. putida* strain (Chang and Hong, 1994). Analysis of effluent streams from a 1 m³ fixed bed bioreactor also showed that dissolved elemental mercury concentrations in the effluent were very low (< 5%), while 60-80% of the mercury was bound to biomass (Leonhäuser et al., 2006).

Hg(II) transformation by *P. putida* Spi3 in continuous culture

The naturally mercury-resistant strain *P. putida* Spi3 was studied under similar conditions. Dilution rate was kept constant ($D = 0.1 \text{ h}^{-1}$) and the Hg(II) inflow concentration was varied from 10 mg L⁻¹ to 500 mg L⁻¹. As shown in Figure 2 the time courses of the bio dry mass and the mercury transformation capacity were comparable with the strain KT2442::*mer73*. However, the concentration of total and soluble Hg in the effluent was higher for Spi3 than for KT2442::*mer73*. In spite of this a high mercury removal efficiency of

98.5% and more was reached. As observed with the strain KT2442::*mer73*, there was a significant difference between $c_{\text{Hg,T,out}}$ and $c_{\text{Hg,S,out}}$. A drastic increase in the mercury effluent concentration was observed at a Hg(II) inflow concentration of 500 mg L^{-1} . The total mercury effluent concentration increased to 95 mg L^{-1} (1.54 mg L^{-1} soluble Hg) but the activity of the microbes was not affected, as indicated by the constant BDM and the oxygen consumption. As reported before (Leonhäuser et al., 2006), Hg(II) transformation by *P. putida* is subjected to substrate (Hg(II)) inhibition and a soluble Hg(II) concentration of 1.54 mg L^{-1} in the culture medium was shown to be inhibitory. This indicates that the Hg concentration of 95 mg L^{-1} detected in the effluent must have been bound to the cell surface and not have been bioavailable. Otherwise the microbial cells would not have survived in such a toxic environment.

Proteome analysis of the two *P. putida* strains under high Hg(II) loads

Proteome analysis was conducted to determine first, how the expression of the *mer* operon was regulated under different Hg(II) loads in the naturally mercury resistant strain Spi3; second, whether the high Hg(II) loads applied presented stress for the cells of the two strains despite the presence of a resistance mechanism; and third, whether the need for reduction equivalents during Hg (II) transformation required adaptations of the energy metabolism of the organism, especially under high Hg(II) load conditions.

At first, *P. putida* KT2442::*mer73* was studied to adapt the 2-DE/MS method established before in our laboratory for the proteome analysis of other microorganisms (Wang et al. 2003a, 2003b, 2005). Typical protein expression patterns obtained from 2-D IEF/SDS-PAGE gel electrophoretic separation of an intracellular protein extract in the pH ranges of 4-7 and 6-11 are presented in Figure 3. Approximately 550 to 650 spots could be visualized in the pH range of 4-7 and around 80-100 spots in the pH range of 6-11, of which 248 and 53 spots, respectively, were subjected to in-gel digestion with trypsin and analysed by MALDI-

TOF/MS. By peptide mass fingerprinting (PMF) against the specific protein database of *P. putida* KT2442, 224 out of the 248 acidic protein spots as well as 50 out of the 53 basic protein spots were identified.

Since proteins encoded by the genes of the *mer* operon are non-intrinsic proteins of *P. putida* KT2442, they can not be identified through PMF against the specific protein database of *P. putida* KT2442. Fortunately, all the proteins of the *mer* operon from the *Serratia marcescens* plasmid pDU1358 as well as the *merA* genes of the strain *P. putida* Spi3 have already been sequenced (Felske et al. 2003). Therefore, peptide masses of protein spots that were not identified first by PMF against the protein database of *P. putida* KT2442 were compared with these known protein sequences using the BLAST function of the BioEdit program (<http://www.mbio.ncsu.edu/BioEdit/bioedit.html>). The sequence alignment results were verified using partial protein sequences obtained from ESI-QqTOF MS/MS analysis as described before (Wang et al., 2005) to search for homologue proteins against the public protein database NCBIInr with the MASCOT search engine (<http://www.matrixscience.com/>).

Then, *P. putida* Spi3 was studied. The genome of this strain has not yet been sequenced except its *merA* genes. Protein identification was realized by using data from MALDI-TOF MS and ESI-QqTOF MS/MS analyses to search for homologous proteins in the public protein database NCBIInr which contains also protein sequences of *P. putida* KT2442.

Samples from different Hg(II) loads of the two *P. putida* strains used for proteome analysis are indicated in Figure 2 and listed in Table3 with their characteristic mercury concentrations in the inflow and in the effluent. It should be mentioned that all samples were taken under steady state conditions, except S2 which was taken 2 hours after starting the mercury feed at $c_{\text{Hg,in}} = 10 \text{ mg L}^{-1}$ but before reaching the steady state conditions. For sample P3 of KT2442::*mer73* and sample S6 of Spi3 residual concentrations of 0.032 and 0.490 mg Hg(II) L⁻¹, respectively, were detected (Table3) after the Hg(II) inflow was already stopped. They probably resulted from the desorption of mercury from the biofilm on the reactor wall.

Mercury resistance proteins

Despite the effort to extract the cellular proteins with a lysis buffer of enhanced solubility for hydrophobic proteins, capture of the very basic and hydrophobic MerP and MerT proteins failed. So far only MerA and MerB were identified. For the strain KT2442::*mer73* three spots were unambiguously identified as MerA (MerA-I, MerA-II and MerA-III) (Figure 4), although KT2442::*mer73* possesses only one *merA* gene. Thus, the appearance of more than one spot of MerA probably resulted from posttranslational modifications or modifications occurring during 2-DE analysis. Similarly, two spots were identified as MerB (MerB-I and MerB-II) (Figure 4). MerA-I belonged to the highly expressed proteins, accounting for 3.5-4.2% of the total protein amount detected in the pH range of 4-7. MerB-I also belonged to the highly expressed proteins, comprising about 2% of the total protein amount detected. Under high Hg(II) loads expression of the three MerA spots and the two MerB spots remained constant within the quantification error range (Figure 4 and Figure 5). The independence of the expression of MerA and merB from Hg(II) concentration was expected, since these genes are under the control of a strong and constitutively active promoter for the alanyl-tRNA-synthase gene (Pauling 2003).

Four spots of MerA and MerB, respectively, were identified for the strain Spi3 (Figure 4), for which significant changes in expression levels were observed in the samples analyzed with different Hg(II) loads (Figure 6). In sample S1 no mercury was fed and the expression of MerA protein was hardly detectable. When the mercury feeding was started (sample S2) the expression of MerA was clearly increased. and it increased even further as the Hg(II) load increased, reaching a maximum expression level at a Hg(II) inflow concentration of 200 mg L⁻¹. A further increase of the Hg(II) inflow concentration to 500 mg L⁻¹ did not result in an additional increase in the expression level of MerA. The maximum expression level of MerA in Spi3 was similar to that found for KT2442::*mer73* at all mercury concentrations (Figure 4

and Figure 6). After the mercury feed was stopped (sample S6) the expression of MerA decreased but was still much higher than that found for sample S1, because the remaining soluble Hg in the culture medium was still 0.49 mg L^{-1} (Table 3). Thus, in Spi3 the expression of the MerA protein was strongly dependent on the Hg(II) load, or more specifically, on the soluble Hg concentration. The soluble Hg represents the fraction of the total Hg concentration which is actually bioavailable for the cells and this is able to induce a cellular response. Despite the absence of organic mercury compounds in the culture medium, MerB was also expressed with a time course similar to that of MerA (Figure 4 and Figure 6). This is because that *merA* and *merB* genes of Spi3 are regulated by the same promoter, and their translation apparently is also regulated in a similar way

The soluble Hg concentrations determined in this study are several orders of magnitude above the concentrations known for the induction of gene transcription of the *mer* operon in different microorganisms such as *E. coli* and *Vibrio anguillarum* (Ralston and O'Halloran, 1990; Golding et al., 2002; Kelly et al., 2003). According to what has been reported, induction of the *mer* operon transcription is characterized by a hypersensitive response (“ready to rock”) across a very narrow range of Hg(II) concentrations in the picomolar range and occurs within 30 sec. Thus, if this kind of *mer* operon induction exists also in *P. putida* Spi3 and if the mRNAs is readily translated to the corresponding proteins, theoretically, full induction of the *mer* operon transcription and translation should have been completed already for sample S2, i.e. 2 h after switching the chemostat from no Hg (II) inflow to an Hg(II) inflow of 10 mg L^{-1} . What we have observed, however, was a further increases in the expression of MerA and MerB within a time period of approximately 24 h at a constant Hg(II) inflow concentration of 10 mg L^{-1} but with an increase of the soluble Hg concentration from $78 \text{ } \mu\text{g L}^{-1}$ to $130 \text{ } \mu\text{g L}^{-1}$ (Figure 6, sample S2 vs. sample S3). In addition, the expression of the MerA and MerB proteins was further unregulated as the soluble Hg concentration increased to $480 \text{ } \mu\text{g L}^{-1}$ (Figure 6, sample S3 vs. sample S4). Thus, the proteome data clearly show a concentration-

dependent expression of *merA* and *merB* proteins. The discrepancy between the reported mechanism of induction of the *mer* operon and the protein expression data shown here might result from differences between regulation at the transcriptional level and at the translational level. It is well known for prokaryotic gene regulation that the cell can "turn off" the synthesis of proteins from its DNA in several ways, e.g. the cell could selectively degrade a mRNA as soon as it was made to prevent it from being translated into protein, or the cell could selectively prevent translation of an otherwise stable mRNA. To clarify this question, a simultaneous analysis of the transcription and translation of the *mer* operon needs to be carried out. However, the transcription of the *mer* operon genes in *P. putida* Spi3 could be also controlled by a novel, as yet unknown regulatory mechanism which does not show the on/off type of induction reported before but is finely tuned to the actually available Hg(II) concentration. It should be mentioned that *P. putida* Spi3 harbours several *mer* operons which differ in operon structure and include two variants of *merA* and *merB* with different sequences (Fehr 2006) and possibly also different mechanisms of regulation. More detailed investigations on the expression of the different *mer* operons of *P. putida* Spi3 in the chemostat would be required to clarify this question, e.g. by using reporter strains with *gfp-merA* fusions and analysing gene expression on a single cell level.

In addition to the different expression patterns of MerA and MerB described above, general cellular responses of the two *P. putida* strains to high Hg(II) loads showed also certain differences as can be directly visualized in Figure 7. Significantly up- and downregulated proteins are summarized in Table 4 and some of them are discussed in detail below.

Cellular response of KT2442::mer73 to high Hg(II) loads

Central carbon metabolism and energy metabolism

Although about 550 to 650 spots and 80 to 100 spots can be visualized in the pH range of 4-7 and 6-11, respectively, the majority of them did not show significant changes (more

than twofold up- or downregulation) in their expression after the Hg(II) inflow concentration was increased from 10 mg L⁻¹ to 200 mg L⁻¹, as demonstrated in Figure 3. This includes most enzymes of the central carbon metabolism (glycolysis/gluconeogenesis, pentose phosphate pathway, and TCA cycle), indicating a metabolic steady-state.

Increased energy demand under high Hg(II) load might be required to satisfy the need of providing the reduction equivalent NADPH₂ for reducing Hg(II) to Hg(0). We have identified a lot of enzymes involved in energy metabolism, such as several NADH dehydrogenases (NuoCD, NuoF, NuoG), a quinone oxidoreductase (PP0072), two electron transfer flavoproteins (PP4201 and PP4203), alpha, beta, delta and gamma subunits of the ATP synthase F1 complex (AtpA, AtpB, AtpG and AtpH). However, except AtpG (PP5414) which showed a 2.2-fold increase at higher Hg(II) load, none of them showed any significant alterations in their expression levels regardless of clearly changed Hg(II) load. The TCA cycle enzyme isocitrate dehydrogenase (PP4011) which uses ATP to synthesize NADPH from NADP(+) showed even a 3.0-fold decrease in its expression level at high Hg(II) inflow concentration. Thus, the proteome analysis did not indicate any increased energy demand at high Hg(II) load.

Protein synthesis

Several enzymes for amino acid synthesis and metabolism were affected (Table 4). Interestingly, while glutamate synthase (PP1037) was 3.2-fold upregulated, glutamine synthase (PP5046) was downregulated 5.1-fold. KT2442::*mer73* has the *merTPAB* genes inserted into the alanyl-t-RNA synthase gene (Pauling 2003), which is present in monocopy. Inactivation of the alanyl-t-RNA synthase gene may change the pool of available t-RNAs that bind and transport alanine for protein synthesis. Consequently alanine might accumulate and inhibit as one of the allosteric inhibitors the activity of glutamine synthetase. The upregulation

of glutamate synthase might be needed to maintain the pool of the two compatible solutes glutamine and glutamate in the cytosol.

Basic ribosomal proteins make up a great part of the proteome in the pH range of 6-11. 6 of these ribosomal proteins were upregulated (between 2.0-fold and 11-fold) at high Hg(II) load, indicating a generally enhanced protein synthesis under the stress conditions caused by high Hg(II) load.

Membrane-related transport, stress response

Remarkable changes in protein expressions of KT2442::*mer73* were observed for some membrane transport and binding proteins. A very interesting expression pattern was found for one component of a sugar ABC transporter, a periplasmic sugar-binding protein (PP1015) which functions to transport carbohydrates, organic alcohols, and acids across the cell membrane. This sugar-binding protein showed four isoforms. Two of them (PP1015-I and PP1015-II) belonged to the highly expressed proteins, accounting for over 5% and 4%, respectively, of the total protein amounts determined. Interestingly, expression changes of these two isoforms were not consistent with each other. While PP1015-I was down-regulated at increased Hg(II) inflow, PP1015-II showed clearly elevated expression at higher Hg(II) inflow concentration (Figure 8). The expression levels of the other two isoforms were relatively low, with PP1015-III showing changes similar to PP1015-II and PP-1015-IV similar to PP1015-I. All these four isoforms appeared to have similar molecular weights but quite different *pI* values. It is well known that protein isoforms with different *pI* values can result from posttranslational modifications such as phosphorylation. Activities of many enzymes are controlled by their phosphorylation or dephosphorylation levels. Therefore, it is conceivable that PP1015-I and PP1015-III might represent the phosphorylated and dephosphorylated forms of the sugar binding proteins, respectively and thus the ABC transporter appears to tune its activity through changes in its

phosphorylation/dephosphorylation ratio. To verify this hypothesis, further investigation through e.g. phosphoproteome analysis need to be carried out. Another sugar ABC transporter (PP1018), which is assigned a function similar to PP1015, demonstrated increased expression with increased Hg(II) inflow and decreased expression after the feeding of mercury was turned off. Although the substrate specificities of these transporters are still unknown, the result seems consistent with the cultivation conditions of *KT2442::mer73* in a minimal medium with glucose as the sole carbon and energy source, and indicate higher demand on nutrients and energy at higher Hg(II) load.

A periplasmic iron-binding protein of a putative iron ABC transporter (PP5196) was found to be strongly (17.5-fold) up-regulated after switching the Hg(II) inflow from 10 mg L⁻¹ to 200 mg L⁻¹, then was down-regulated about 6-fold after the stop of mercury feeding, indicating perhaps a higher demand of the cells for iron-uptake from the medium under high Hg(II) load.

Two transmembrane proteins with porin activity, namely porin D (OprD, PP1206) and the outer membrane protein OprF (PP2089) were remarkably up-regulated 5.6-fold and 21.5-fold respectively at elevated Hg(II) inflow concentrations, then down-regulated 3.2-fold and 19-fold, respectively, after the Hg(II) feeding was shut down. Porins are known to associate as trimers to form aqueous channels that aid the passive transport (diffusion) of small hydrophilic molecules, such as nutrients or cell waste products, across the outer membrane of Gram-negative bacteria. Perhaps OprD and OprF were involved in either the inward diffusion of Hg(II) into the cells or in the outward diffusion of Hg(0) out of the cells or in both processes.

Expression of a putative betaine-aldehyde dehydrogenase (PP0708) was strongly increased about 14-fold after the Hg(II) inflow was increased from 10 mg L⁻¹ to 200 mg L⁻¹, then decreased for 6-fold after switching off the Hg(II) inflow. This enzyme is involved in the

second step of the biosynthesis of the osmoprotectant betaine from coline, indicating probably higher osmotic stress at higher Hg(II) inflow concentration.

It can be concluded that high Hg(II) load generally resulted in elevated membrane-related transport activities and potentially osmotic stress to the cell.

Cellular response of Spi3 to high Hg(II) loads

No significant changes in the expression of enzymes related to central carbon metabolism, energy metabolism, and protein synthesis were found in Spi3.

The proteins affected most strongly by high Hg(II) loads in Spi3 were related to membrane transport as in KT2442::*mer73*. However, in contrast to the upregulation of OprD (PP1206) and OprF (PP2089) in KT2442::*mer73*, expression of OprD (PP1206) was drastically downregulated (106-fold) in response to high Hg(II) load in Spi3. The expression of OprF (PP2089) was downregulated as well but to a less extent (2-fold). Such strong downregulation may indicate a specific defence reaction of the cell to protect it from the inward diffusion of Hg(II) into the periplasma. On the other side expression of a putative porin (PP0046) was found to be strongly upregulated at high Hg(II) load. Actually, it was only detectable when the Hg(II) load reached 200 mg L⁻¹ and increased further (2-fold) as the Hg(II) load rose to 500 mg L⁻¹. Its expression was strongly downregulated (19-fold) after the Hg(II) inflow was stopped (Table 4). This result probably reflects the need of the cell to allow the outward diffusion of metabolic waste products at high Hg(II) load. Interestingly, the expression level of an efflux protein for cobalt/zinc/cadmium (PP0044) was increased 39-fold at a Hg(II) load of 200 mg L⁻¹ or 45-fold when the Hg(II) load reached 500 mg L⁻¹. Although this protein is annotated as an efflux pump for cobalt/zinc/cadmium, it may well have the ability to transport also other divalent heavy metals, e.g. Hg(II), and thus be part of a global cellular resistance mechanism of the cell against heavy metals including mercury. It has to be mentioned that the sugar ABC transporter (PP1015) that was found to be one of the

highly expressed protein in KT2442::*mer73* was not found in the proteome of Spi3 in any of the samples analyzed. Expression of another sugar ABC transporter (PP1018) showed no clear correlation with the Hg(II) inflow or effluent concentrations (Table 4). Increased expression of the putative iron ABC transporter (PP5196) was also not found in Spi3.

Interestingly, two spots which were identified as a catalase/oxidase (PP3668), were strongly downregulated (up to 51-fold) in responses to higher Hg(II) load, then upregulated again after the turnoff of Hg(II) inflow. This protein can neutralize potentially lethal hydrogen peroxide molecules in many archaeal and bacterial organisms. Its role under the experimental conditions applied in this study is presently not known, but assuming that it exerts similar function in *P. putida* spi3, the data indicate less oxidative stress at higher Hg(II) load.

Concluding remarks

This study showed that extremely high Hg(II) concentrations of up to 500 mg L⁻¹ can be successfully transformed to Hg(0) with an efficiency of up to 99.9% by the genetically engineered strain KT2442::*mer73*, as well as by the natural mercury resistant isolate *P. putida* Spi3. However, the concentration of particle bound mercury increased strongly especially for the strain Spi3. In this case biomass removal by means of a retention device, e.g. a membrane filter, is necessary to treat mercury contaminated wastewater with high efficiency.

In general, proteome analysis showed that the cellular responses of the two strains of *P. putida* strains towards high Hg(II) loads were small with regard to central carbon metabolism and energy metabolism. There was no indication of increased energy demand for the transformation of Hg(II) to Hg(0) even at a Hg(II) load up to 500 mg L⁻¹ under chemostat cultivation conditions. While constant expression was confirmed for the MerA and MerB proteins, which are under the control of a strong and constitutively expressed promoter in the recombinant strain KT2442::*mer73*, their expression showed a strong dependence on the Hg(II) concentration in the naturally mercury-resistant strain Spi3. Both strains demonstrated

remarkable but quite different alterations in membrane related transport activities in response to high Hg(II) loads. Spi3 showed specific detoxification reactions beyond the induction of the *mer* operon, e.g. the upregulation of a cation efflux pump and the downregulation of an outer membrane porin, presumably resulting in reduced diffusion of Hg(II) into the cell and increased active efflux at the same time.

References

- Barkay, T., Wagner-Döbler, I. (2005). Microbial Transformation of Mercury: Potentials, Challenges and Achievements in Controlling Mercury Toxicity. *Adv. Appl. Microbiol.* 57:1-52
- Barkay, T., Miller, S.M., Summers, A.O. (2003). Bacterial Mercury Resistance from Atoms to Ecosystem. *FEMS Microbiol. Rev.* 27:355-384
- Becker, F.U. (1996). Stofftransportraten und Reaktionsgeschwindigkeiten der Hg-Biotransformation in Mehrphasenreaktoren. Dissertation TU Braunschweig, *Cuvillier Verlag*, Göttingen
- Chang, J.-S., Hong, J. (1994). Biosorption of Mercury by Inactivated Cells of *Pseudomonas aeruginosa* PU21 (Rip64). *Biotech. Bioeng.* 44:999-1006
- Deckwer, W.-D, Becker, F. U., Ledakowicz, S., Wagner-Döbler, I. (2004). Microbial Removal of Ionic Mercury in a Three-Phase Fluidized Bed Reactor. *Environ. Sci. Technol.* 38:1858-1865
- EPA U.S. Environmental Protection Agency (1997). Mercury Study Report to Congress, Volume II: An Inventory of Anthropogenic Mercury Emissions in the United States. Office of Air Quality Planning and Standards and Office of Research and Development, EPA-452/R97-003
- European Union (2001). Ambient Air Pollution by Hg. Position Paper
- Fehr, W. (2006). Biotransformation of Thiomersal by Naturally Mercury Resistant Isolates and Genetically Engineered Microorganisms. Dissertation, TU Braunschweig
- Felske, A., Fehr, W., Pauling, B.V., von Canstein, H., Wagner-Döbler, I. (2003). Profiling Mercuric Reductases (*merA*) in Biofilm Communities of a Technical Scale Biocatalyser. *BMC Microbiology* 3:22

Golding, G.R., Kelly, C.A., Sparling, R., Loewen, P.C., Rudd, J.W.M., Barkay, T. (2002). Evidence for Facilitated Uptake of Hg(II) by *Vibrio anguillarum* and *Escherichia coli* under anaerobic and aerobic conditions. *Limnol. Oceanog.* 47:697-975

Heaven, S., Ilyushchenko, M. A., Tanton, T. W., Ullrich, S. M., Yanin, E. P. (2000). Mercury in the River Nura and its Floodplain, Central Kazakhstan: I. River sediments and water, *Sci. Total. Environ.* 260:35-44

Horn J. M., Brunke, M., Deckwer, W.-D., Timmis, K.N. (1994). *Pseudomonas putida* Strains which Constitutively Overexpress Mercury Resistance for Biodegradation of Organomercurial Pollutants. *Appl. and Environ. Microbiol.* 60:357-362

Kelly, C.A., Rudd, J.W., Holoka, M.H. (2003). Effect of pH on Mercury Uptake by an Aquatic Bacterium: Implications for Hg Cycling. *Environ. Sci. Technol.* 37:2941-2946

Lamanda, A., Zahn, A., Roder, D., Langen, H. (2004) Improved Ruthenium II tris (bathophenanthroline disulfonate) staining and destaining protocol for a better signal-to-background ratio and improved baseline resolution. *Proteomics.* 4(3):599-608

Leonhäuser, J., Röhricht, M., Wagner-Döbler, I., Deckwer, W.-D. (2006). Reaction Engineering Aspects of Microbial Mercury Removal. *Eng. Life Sci.* 6:139-148

Misra, T.K. (1992). Bacterial Resistances to Inorganic Mercury Salts and Organomercurials. *Plasmid.* 27:4-16

Nies, D.H. (1999). Microbial heavy-metal resistance. *Appl. Microbiol. Biotechnol.* 51:730-750

Pauling, B.V. (2003). Impact Investigation of a Mercury Reducing GEM in Stream Microcosms & Construction of Mercury Reducing Reporter Strains Based on the Safety Strain *Ps. putida* KT2440. Dissertation, TU Braunschweig

Rabilloud, T., Strub, J.M., Luche, S., van Dorselaer, A., Lunardi, J. (2001) A comparison between Sypro Ruby and ruthenium II tris (bathophenanthroline disulfonate) as fluorescent stains for protein detection in gels. *Proteomics.* 1(5):699-704

- Ralston, D.M., O'Halloran, T.V. (1990) Ultrasensitivity and Heavy-metal Selectivity of the Allosterically Modulated MerR Transcription Complex. *Proc. Natl. Acad. Sci. USA* 87:3846-3850
- Silver, S., Phung, L.T., (1996). Bacterial Heavy Metal Resistance: New Surprises. *Annu. Rev. Microbiol.* 50:753-789
- von Canstein H., Li, Y., Timmis K.N., Deckwer, W.-D., Wagner-Döbler, I. (1999). Removal of Mercury from Chloralkali Electrolysis Wastewater by a Mercury-Resistant *Pseudomonas putida* Strain. *Appl. Environ. Microbiol* 65:5279-5284
- Wagner-Döbler I., von Canstein, H., Li, Y., Timmis, K. N., Deckwer, W.-D. (2000). Removal of Mercury from Chemical Wastewater by Microorganisms in Technical Scale. *Environ. Sci. Technol.* 34:4628-4634
- Wagner-Döbler I., von Canstein, H., Li, Y., Leonhäuser, J., Deckwer, W.-D. (2003). Process-Integrated Microbial Mercury Removal from Wastewater of Chlor-Alkali Electrolysis Plants. *Eng. Life Sci.* 4:177-181
- Wang, W., Sun, J., Hartlep, M., Deckwer, W.-D., Zeng, A.-P. (2003). Combined use of proteomic analysis and enzyme activity assays for metabolic pathway analysis of glycerol fermentation by *Klebsiella pneumoniae*. *Biotechnol Bioeng.* 83(5):525-36
- Wang, W., Sun, J., Nimtz, M., Deckwer, W.-D., Zeng, A.-P. (2003). Protein identification from two-dimensional gel electrophoresis analysis of *Klebsiella pneumoniae* by combined use of mass spectrometry data and raw genome sequences. *Proteome Sci.* 1(1):6
- Wang, W., Hollmann, R., Furch, T., Nimtz, M., Malten, M., Jahn, D., Deckwer, W.-D. (2005) Proteome analysis of a recombinant *Bacillus megaterium* strain during heterologous production of a glucosyltransferase. *Proteome Sci.* 3:4
- Wang, W., Sun, J., Hollmann, R., Zeng, A.-P., Deckwer, W.-D. (2006). Proteomic characterization of transient expression and secretion of a stress-related metalloprotease in high cell density culture of *Bacillus megaterium*. *J. Biotechn.* 126:313-324

Figure Legends

Figure 1: Schematic experimental setup of the continuous stirred tank reactor

Figure 2: Hg(II) transformation in a continuous stirred tank reactor with *P. putida* KT2442::*mer73* (A) and *P. putida* Spi3 (B) at various Hg(II) inflow concentrations. $D = 0.1 \text{ h}^{-1}$, glucose concentration at inflow 4 g L^{-1} , aeration rate 1 vvm, $pO_2 > 50\%$, $T = 30^\circ\text{C}$, $pH = 7$. P1 - P3 and S1 – S6 are samples used for proteome analysis.

Figure 3: 2-D IEF/SDS-PAGE gel electrophoretic separation of an intracellular protein extract of *P. putida* KT2442::*mer73* in the pH range of 4 – 7 (A) and pH range 6 – 11 (B). Cell samples were taken from the chemostat culture at high Hg(II) load (sample P2).

Figure 4: Enlarged view of the protein spots changes of MerA (A) and MerB (B) on 2-D gels for KT2442::*mer73* and Spi3 from samples taken at different Hg(II) loads

Figure 5: Expression of MerA (A) and MerB (B) in *P. putida* KT2442::*mer73* at various Hg(II) loads

Figure 6: Expression of MerA (A) and MerB (B) in *P. putida* Spi3 at various Hg(II) loads

Figure 7: Different protein expression patterns of *P. putida* KT2442::*mer73* (A) and Spi3 (B) in the pH range of 4-7. Both samples were taken from the chemostat culture at a Hg(II) load of $c_{\text{Hg,in}} = 200 \text{ mg L}^{-1}$.

Figure 8: Different expression behavior of the four isoforms of the periplasmic sugar binding protein PP1015 in *P. putida* KT2442::*mer73*.

Tables

Table 1: Characterization of the proteins (pI, Mr and GRAVY) encoded by the genes of the *mer* operon of *P. putida* KT2442::*mer73*

Protein	Isoelectrical Point pI	Molecular Mass Mr (Da)	Hydropathicity GRAVY
MerA	5.80	58711	0.060
MerB	5.67	23078	0.068
MerP	9.43	9548	0.240
MerT	9.34	12511	0.958

Table 2: Hg(II) transformation in a continuous stirred tank reactor (C-limited) with *P. putida* KT2442::*mer73* at various dilution rates and Hg(II) inflow concentrations. Glucose at inlet 4 g L⁻¹, aeration rate: 1 vvm, pO₂ = 50% of saturation

D (h ⁻¹)	X (g L ⁻¹)	c _{Hg,in} (mg L ⁻¹)	c _{Hg,S,out} (mg L ⁻¹)	c _{Hg,T,out} (mg L ⁻¹)	Hg-Removal (%)	R _{Hg v} (mg L ⁻¹ h ⁻¹)	R _{Hg x} (mg g ⁻¹ _{BDM} h ⁻¹)
0.1	1.4	10	0.02	0.07	99.8	0.99	0.71
0.1	1.8	50	0.06	0.18	99.9	4.99	2.77
0.1	1.7	100	0.08	0.20	99.9	9.98	5.87
0.1	1.7	200	0.09	0.19	99.9	19.98	11.75
0.2	1.4	10	0.02	0.07	99.8	1.98	1.41
0.3	1.6	10	0.02	0.07	99.8	2.97	1.86

Table 3: Hg(II) inflow and effluent concentrations of the samples used for proteome analysis from the chemostat culture with *P. putida* KT2442::*mer73* and Spi3

Sample No.	$C_{\text{Hg,in}}$ [mg L ⁻¹]	$C_{\text{Hg,S,out}}$ [mg L ⁻¹]
<i>KT2442::mer73</i>		
P1	10	0.015
P2	200	0.085
P3	0	0.032
<i>Spi3</i>		
S1	0	0.000
S2	10	0.078
S3	10	0.130
S4	200	0.480
S5	500	1.540
S6	0	0.490

Table 4: Significant changes (at least 2-fold) in cellular protein expressions of *P. putida* in response to the increased mercury load (P2 vs P1 for KT2442::*mer73* and S4 vs S1 for Spi3), as well as to the decreased mercury load (P3 vs P2 for KT2442::*mer73* and S6 vs S4 for Spi3)

Protein	Ordered Locus Names (<i>P. putida</i> KT2440)	Regulation (fold)			
		KT2442:: <i>mer73</i>		Spi3	
		P2 vs P1	P3 vs P2	S4 vs S1	S6 vs S4
Transport Proteins					
Cobalt / zinc / cadmium efflux	PP0044			+ 38.6	- 2.9
Outer membrane porin, putative	PP0046			++	- 19.1
Outer membrane porin, putative	PP1206	+ 5.6	-3.2	-106.3	--
Outer membrane protein OprF	PP2089	+ 21.5	- 19.1	- 2.0	- 2.0
Sugar ABC transporter, periplasmic binding protein	PP1015	up to + 6.5	- 1.6	n.d.	n.d.
Sugar ABC transporter, ATP binding subunit	PP1018	+ 2.0	-1.4		
Putrescine ABC transporter, periplasmic putrescine-binding protein	PP5181			-3.0	+ 3.3
Iron ABC transporter, periplasmic iron-binding protein, putative	PP5196	17.5	- 6.3		
Amino acid synthesis and metabolism					
Glutamate Synthase	PP4037	+ 3.2	No change		
Glutamine Synthetase	PP5046	- 5.1	- 2.4		
Tryptophan Synthase	PP0082	+ 3.0	No change		
Serine hydroxymethyltransferase	PP0671	-5.4	+ 3.0		
Ornithine carbamoyltransferase	PP1000			- 8.0	+ 3.5
Arginine deiminase	PP1001	-17.5	+ 8.1		
TCA Cycle					
Fumarate Hydratase	PP0897	- 5.2	+ 4.2		
Isocitrate Dehydrogenases	PP4011	- 3.0	+ 1.3		

Stress response

Bataine-aldehyde dehydrogenase	PP0708	+ 14.4	- 6.1		
Catalase / Peroxidase	PP3668-I			- 48.1	+ 42.4
	PP3668-II			- 50.6	+ 45.4
60 kDa chaperonin	PP1361			+ 2.3	No change

Energy metabolism

ATP synthase F1, gamma subunit	PP5414	+ 2.2	- 2.0		
--------------------------------	--------	-------	-------	--	--

Glyconeogenesis

Phosphoenolpyruvate synthase	PP2082	- 2.0	No change	- 3.7	+ 2.8
------------------------------	--------	-------	-----------	-------	-------

Protein synthesis

Ribosomal protein L11	PP0443	+ 2.0	- 1.7		
Ribosomal protein S7	PP0450	+ 6.2	- 30.4		
Ribosomal protein L4	PP0455	+ 2.3	- 1.4		
Ribosomal protein L24	PP0465	+ 11.0	- 2.6		
Ribosomal protein L17	PP0480	+ 8.8	- 8.3		
Ribosomal protein L13	PP1315	+ 2.7	- 1.8		

Conserved hypothetical proteins

Conserved hypothetical protein	PP0397			- 6.3	+ 6.5
Conserved hypothetical protein	PP0913			d.	1.1
Conserved hypothetical protein	PP3089			- 12.2	- 16.8
Hypothetical protein	PP1980	+ 3.6	- 3.4		
Hypothetical protein	PP5353	+	-		
